

Lattice QCD with 0, 2 and 4 Quark Flavors

Robert D. Mawhinney*
Columbia University
Department of Physics
New York, NY 10027, USA

November 1, 1996

Abstract

We have done simulations of lattice QCD with different numbers of light dynamical quarks. Since we cannot reach the continuum limit with our current computers, we have done comparisons with 0 (quenched), 2 and 4 light quark flavors with the physical volume and lattice spacing constant, when these are determined from the mass of the rho. We find a 7% (2σ) difference in the nucleon to rho mass ratio for 2 and 4 quarks. More importantly, the effects of chiral symmetry breaking are dramatically decreased for the case of 4 light quarks.

*The two flavor calculation reported here was done at Columbia in collaboration with Shailesh Chandrasekharan, Dong Chen, Norman H. Christ, Weonjong Lee and Decai Zhu. The zero and four flavor calculations were done in collaboration with Dong Chen and Norman Christ at Columbia and Gregory W. Kilcup at the Ohio State University. This work was supported in part by the U.S. Department of Energy. Presented at RHIC Summer Study '96, Brookhaven National Laboratory

1 Introduction

The role of light dynamical quarks in QCD is not fully understood. Perturbatively, light quarks introduce screening and cause the QCD coupling constant to evolve more slowly. The role of light quarks in the low-energy non-perturbative physics of QCD is much less certain. Of major interest in the numerical study of lattice QCD is a qualitative and quantitative determination of light quark effects in low-energy hadronic physics.

In lattice QCD, many calculations have been done in the quenched approximation [1], where the effects of dynamical quarks are removed. Valence quarks can still be introduced, allowing hadron masses to be measured from the decay of two-point hadronic correlation functions, but there are no closed loops involving quarks. Some quenched calculations report hadron masses in reasonable agreement with experiment but what is not known is whether this trend will continue to weaker couplings. In addition, theoretical arguments in the context of chiral perturbation theory have given predictions for specific ways in which the fermion truncation of the quenched approximation will appear; quenched chiral logarithms. If these quenched chiral logarithms appear in numerical results they will certainly cloud the extraction of hadron masses, etc.

Lattice QCD calculations with dynamical fermions are less advanced. Inclusion of the fermionic determinant increases the required computer power by at least 2 orders of magnitude. Over the last few years, calculations on $16^3 \times 32$, $16^3 \times 40$ and 20^4 lattices have been done by a number of groups [1]. However, a full data set with various lattice spacings and volumes is not yet available. To date, very little difference has been seen between the quenched and 2 flavor calculations at zero temperature for similar volumes and lattice spacings. (At finite temperature, differences between the quenched and 2 flavor theories with staggered fermions have been seen for a number of years.)

A study of full QCD comparable to the level of current quenched calculations awaits the coming new computers which will push towards the Teraflop scale. Here we report a less ambitious calculation, which still requires about 7 Giga-flop-years of computing; a comparison of 0, 2 and 4 flavor QCD with a fixed lattice spacing and volume (in units of the rho mass extrapolated to zero valence quark mass). The calculations we report only have results for a single dynamical fermion mass, but we have calculated hadron masses and the chiral condensate for a wide variety of valence quark masses. As we detail

Table 1: Parameters for the three simulations reported here. The run length, thermalization, hadron measurement frequency and jackknife block size are in time units.

	$N_f = 4$	$N_f = 2$	$N_f = 0$
volume	$16^3 \times 32$	$16^3 \times 40$	$16^3 \times 32$
β	5.4	5.7	6.05
$m_{\text{dynamical}} a$	0.01	0.01	
evolution	HMC	HMD	HMC
run length	4450	4870	187,125
thermalization	250	250	375
acceptance rate	0.95		0.91
trajectory length	0.5	0.5	0.75
step size	0.0078125	0.0078125	0.025
CG stopping condition	1.13×10^{-6}	1.01×10^{-5}	
total run time	5 months	7.5 months	1.7 months

below, even from this restricted set of simulations, we have seen pronounced effects of dynamical fermions for the four quark case.

Section 2 gives some details of our calculations. and section 3 details the valence hadron masses we measured for the three simulations and discusses the major differences between them. In section 4 we use a simple model of finite volume effects to support our conclusions about the hadron mass spectrum.

2 Simulation Parameters

We are reporting on three different simulations whose parameters are given in Table 1. The simulations were done using the 16 GigaFlop, 256-node computer at Columbia, which is just finishing its seventh year of full time computation. (Additional quenched simulations were done by Greg Kilcup using the T3D at the Ohio Supercomputer Center. Some results from these are reported in [2].)

All of our simulations were done with staggered fermions. For 0 and 4

flavors, we used an exact hybrid Monte Carlo algorithm, while for 2 flavors, there is no practical exact algorithm available. The R algorithm we employed has “ $(\Delta t)^2$ ” errors, which means observables will have systematic errors of this order, where for our case $\Delta t = 0.0078125$. The high acceptance rate for the exact evolution, which has the same parameters as the inexact evolution (except for the conjugate gradient stopping condition), demonstrates that the $(\Delta t)^2$ errors are negligible for the inexact case.

We have measured hadron correlators using a variety of different source sizes [3], but only report results here from 16^3 wall sources. With staggered fermions, the sinks which are used to select the quantum numbers of the hadronic states can be, and in some cases must be, non-local, due to the fact that the 4 components of the 4 fermionic flavors are delocalized. We have used local sinks for all the hadrons reported here.

3 Results

Figures 1, 2 and 3 are plots of hadron masses as a function of the valence quark mass. In order to compare the plots, a few major points about staggered fermions should be recalled. At any finite lattice spacing, staggered fermions exhibit flavor symmetry breaking. The particles labeled ρ and ρ_2 should become degenerate in the continuum limit and are actually quite degenerate on the lattices we have studied. The a_1 and b_1 correspond to the continuum mesons of the same names, as does the nucleon N . The N' is the parity partner of the nucleon.

The π and π_2 should also be degenerate in the limit of small lattice spacing, but they are far from degenerate for the lattices we studied. An important feature of staggered fermions is the presence of a U(1) chiral symmetry, for finite lattice spacing, when the quark mass is set to zero. (This U(1) symmetry is a subgroup of the $SU(4)_A$ flavor symmetry of four flavor continuum QCD and must not be confused with the anomalous $U(1)_A$ symmetry of the continuum.) This U(1) chiral symmetry of staggered fermions then leads to a Goldstone theorem for the valence pion and the prediction that m_π^2 goes linearly to zero as the valence quark mass goes to zero. Note that it is m_π versus m_{val} plotted here and not m_π^2 , which we will plot later.

The σ particle in these figures is related to the staggered fermion pseudo-Goldstone pion by a U(1) rotation on the valence quark lines. In the contin-

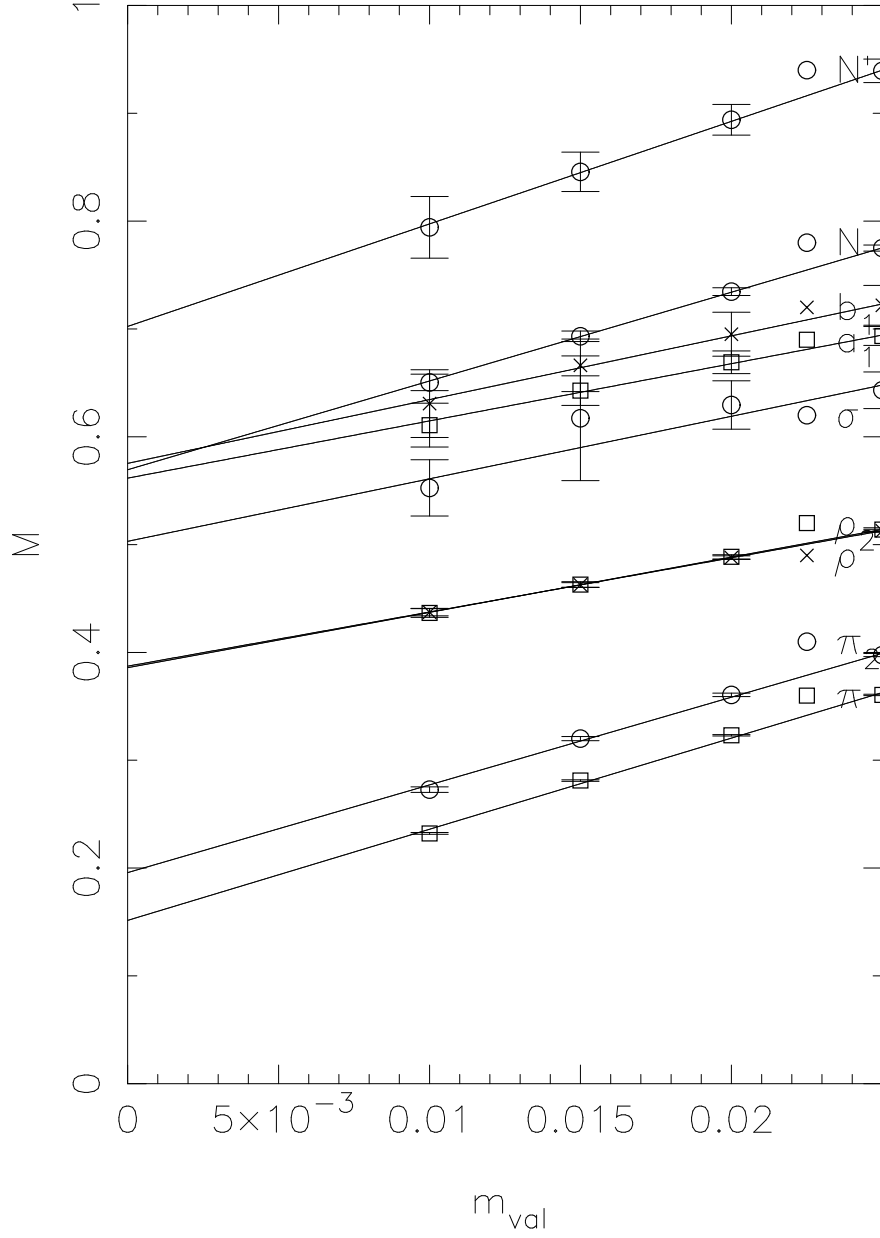


Figure 1: Hadron masses versus m_{val} for the $16^3 \times 32$ quenched calculation at $\beta = 6.05$.

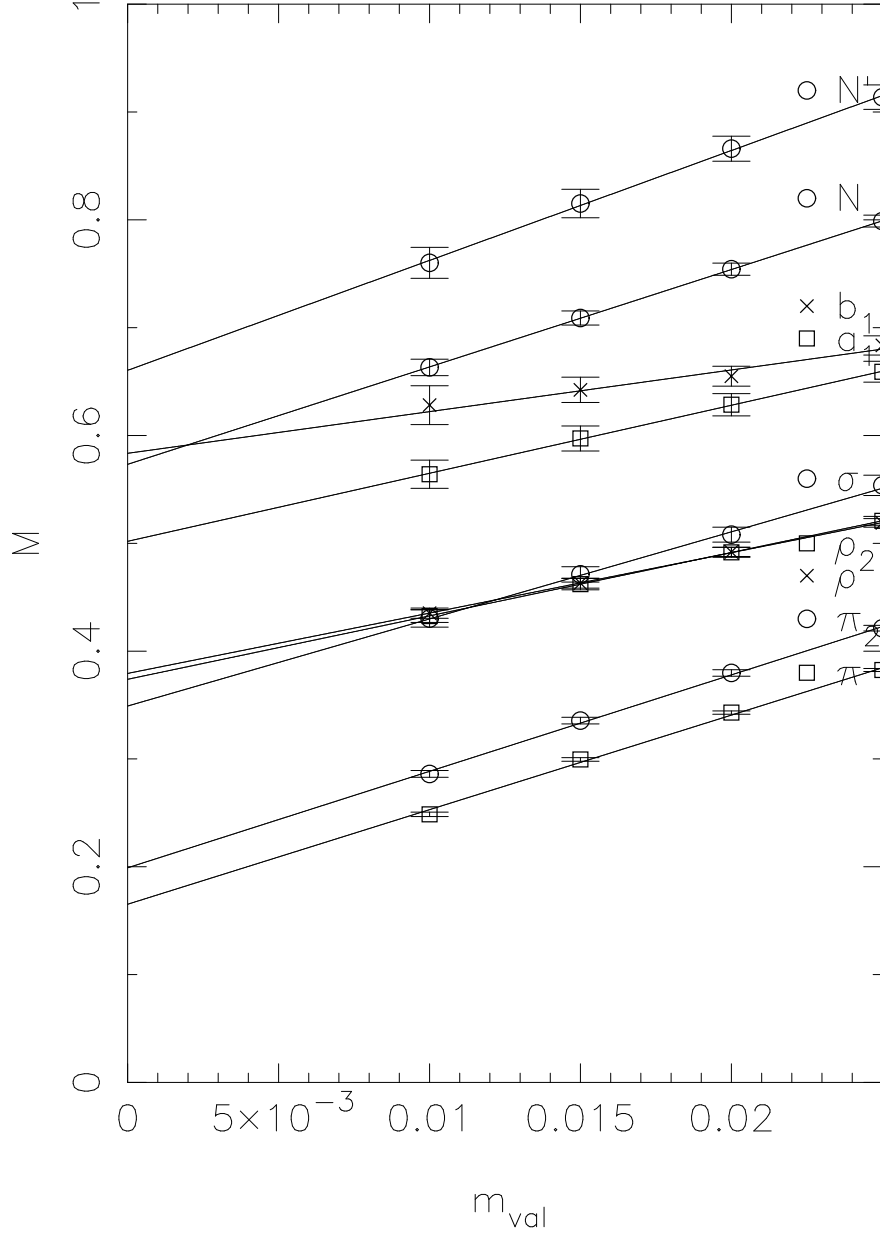


Figure 2: Hadron masses versus m_{val} for the $16^3 \times 40$ two flavor calculation at $\beta = 5.7$ with $m_{\text{dyn}}a = 0.01$.

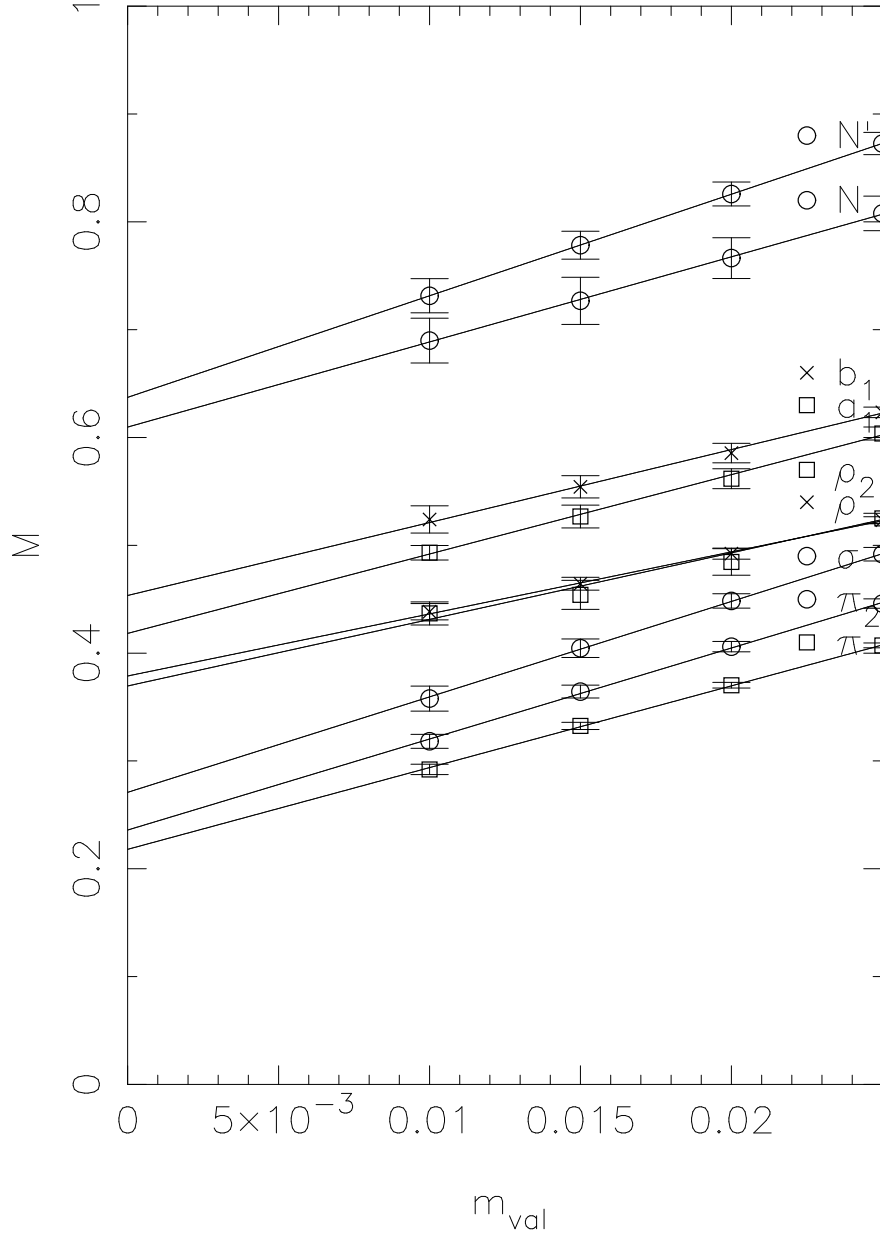


Figure 3: Hadron masses versus m_{val} for the $16^3 \times 32$ four flavor calculation at $\beta = 5.4$ with $m_{\text{dyn}}a = 0.01$.

uum, this σ becomes a scalar, isoscalar particle. However, the σ measured here does not include vacuum bubble contributions. Only quark propagators which start on the source and end on the sink are included in the correlator. This means that for the case where $m_{\text{val}} = m_{\text{dyn}}$, the σ mass reported here is not the mass for the scalar, isoscalar particle for full QCD. However, in the absence of chiral symmetry breaking, this σ and the π are degenerate.

Comparing Figures 1, 2 and 3 reveals the following features:

1. For all three calculations, the values of ρ and ρ_2 agree quite closely for all valence masses and therefore in the extrapolation to $m_{\text{val}} = 0$. The agreement at $m_{\text{val}} = 0$ is a result of our choice of parameters; we wanted to keep the physical volume and lattice size constant in units of the ρ mass. The fact that there is agreement for all valence masses was unexpected.
2. While m_ρ is the same for all three simulations, m_N increases as more quarks are added.
3. The mass of the σ decreases as the number of quark flavors is increased. m_σ is greater than m_ρ for the quenched calculation and clearly less than m_ρ for four flavors.
4. The splitting between parity partners (π, σ) , (ρ, a_1) and (N, N') decreases as the number of dynamical quarks increases. This is evidence for much smaller chiral symmetry breaking effects as the number of dynamical quarks is increased. We will concentrate on this issue in Section 4

The variation in m_N/m_ρ as the number of dynamical quarks is increased is given in Figure 4. There is very little difference between the quenched and 2 flavor calculations for this quantity. This has been seen by others for m_N/m_ρ and is also true of other zero-temperature hadronic quantities like B_K . However, the four flavor calculation is quite distinct from the others. The difference between the 2 and 4 flavor results is about 7% or 2σ . The statistical difference of 2σ does not make an ironclad case for a difference, however as we have varied our statistical analysis this is the smallest statistical difference we have seen.

Another comparison between the three simulations is given in Figure 5, where m_π^2 , m_σ^2 and $m_{\pi_2}^2$ are plotted versus valence quark mass. As mentioned

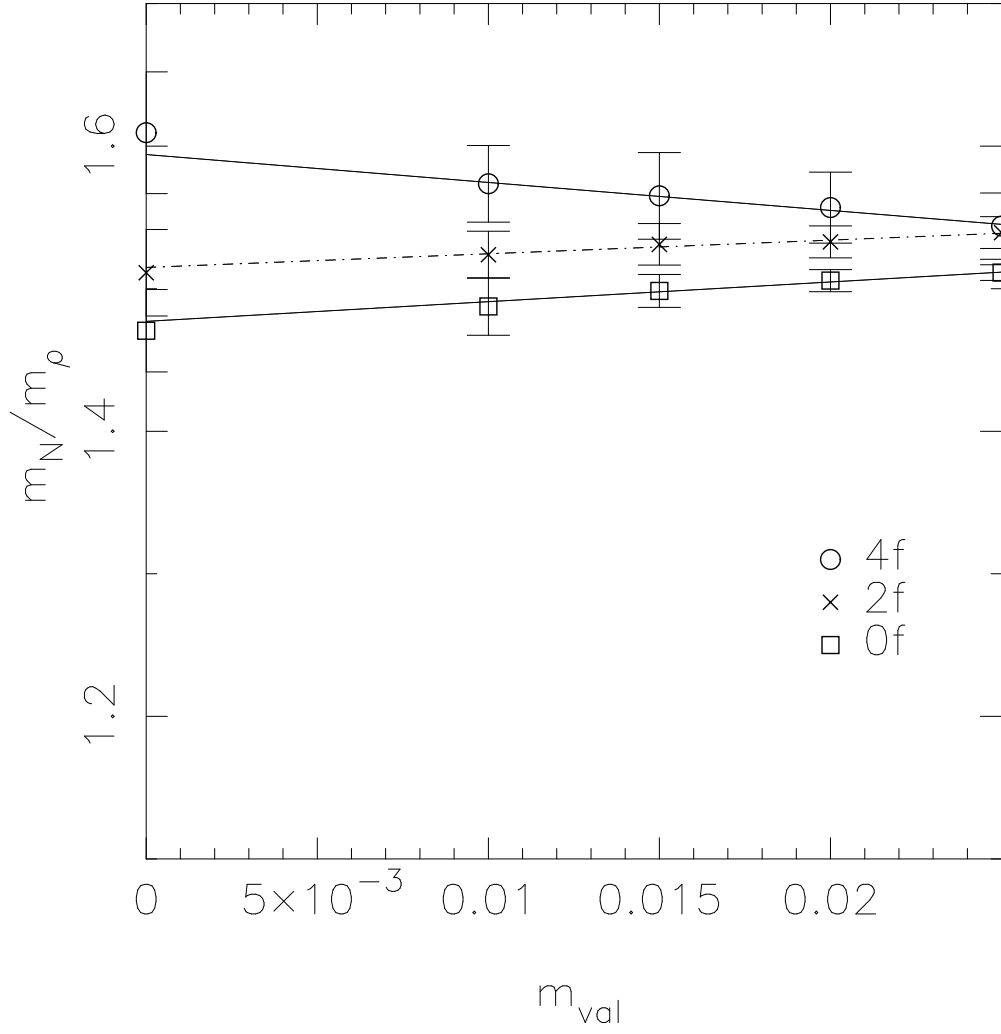


Figure 4: m_N/m_ρ vs. m_{val} for the 0, 2 and 4 flavor calculations. The points at $m_{\text{val}} = 0$ are the ratios of the extrapolated quantities, while the line is the extrapolation of the ratios.

earlier, the presence of a Goldstone theorem for external quark lines means that m_π^2 should go to zero as $m_{\text{val}} \rightarrow 0$. This appears to be the case for the quenched approximation, although the extrapolated value for m_π^2 is actually 6 standard deviations away from zero. For the 2 and 4 flavor calculations, the intercept is growing relatively larger, until for the 4 flavor calculation the intercepts for m_π^2 and m_σ^2 are closer to each other than the intercept for m_π^2 is to zero.

To summarize, we have observed a systematic difference in the value of m_N/m_ρ between four flavors and the other calculations. The remaining features we observe in the valence hadron spectrum are easily understood as a decreased strength of chiral symmetry breaking, except the large intercept for m_π^2 in the limit $m_{\text{val}} \rightarrow 0$. In the next section we use an earlier proposal of ours for finite volume effects to understand this intercept.

4 Chiral Symmetry Breaking and Finite Volume

Before drawing conclusions about the role of light dynamical fermions in four flavor QCD, it is important to be confident that the four flavor simulation we have done has the general qualitative properties associated with the continuum limit of QCD, i.e. confinement and chiral symmetry breaking. There can be unexpected phase structure in theories with many fermions [4], so we seek assurance that we are in a phase consistent with continuum QCD. Evidence for confinement comes indirectly through our hadron mass correlators; we see propagating states that fit the same functional forms as for two flavors where we do have bound hadrons. We have also measured Wilson lines and find no evidence for deconfinement.

As mentioned above the four flavor hadron spectrum shows little effect of chiral symmetry breaking. In addition, extrapolations of m_π^2 to $m_{\text{val}} = 0$ give a large intercept, in apparent contradiction to the Goldstone theorem. This large intercept effect has been known for some time in quenched simulations and was widely expected to be caused by finite volume effects since the intercept became closer to zero as the volume increased. Recently [5], we have proposed a simple model which can help to quantify the role of finite volume effects in quenched or partially quenched calculations. (Our 2 and 4 flavor

calculations are sometimes referred to as partially quenched calculations, since we are discussing valence quark extrapolations on a set of gauge fields that were generated including the effects of quark loops.) To test whether the four flavor results we are seeing are consistent with conventional QCD, we now discuss the role of finite volume effects.

One simple effect of finite volume that has been predicted analytically and is seen numerically is a cutoff in the average eigenvalue density for the Dirac operator. We can observe this effect numerically by measuring the chiral condensate as a function of valence quark mass. In a chirally asymmetric phase, when the valence quark mass is less than the smallest eigenvalue of the Dirac operator, the valence chiral condensate goes to zero linearly with the valence quark mass.

In particular, we write the valence chiral condensate $\langle \bar{\zeta}\zeta \rangle$ as

$$\langle \bar{\zeta}\zeta(m_\zeta) \rangle = 2m_\zeta \int_0^\infty d\lambda \frac{\bar{\rho}(\lambda, \beta, m_{\text{dyn}})}{\lambda^2 + m_\zeta^2} \quad (1)$$

where $\bar{\rho}(\lambda, \beta, m_{\text{dyn}})$ is the ensemble average of the density of eigenvalues of the Dirac operator and m_ζ is the valence mass for the quark fields ζ and $\bar{\zeta}$. (These fields do not enter in the dynamics; they are an extra set of fermions used to probe the system.) The ensemble average can depend on the dynamical fermion mass used (m_{dyn}) as well as $\beta = 6/g^2$. Our normalization is $\int d\lambda \bar{\rho}(\lambda, \beta, m_{\text{dyn}}) = 1$. If $\bar{\rho}(\lambda, \beta, m_{\text{dyn}})$ is zero (or small) below some λ_{min} , then equation (1) gives $\langle \bar{\zeta}\zeta(m_\zeta) \rangle$ going linearly to zero.

To relate this finite volume effect in the quenched chiral condensate to the intercept in the quenched pion mass squared, we use the fact that there is a Gell-Mann–Oakes–Renner relation on the lattice, which is independent of whether the ensemble of gauge fields is quenched or unquenched,

$$C(m_\zeta) = \frac{m_\pi^2(m_\zeta) \langle \bar{\zeta}\zeta(m_\zeta) \rangle}{m_\zeta} \quad (2)$$

where

$$C(m_\zeta) = m_\pi^2(m_\zeta) \int d^4x \langle \pi(x) \pi(0) \rangle \quad (3)$$

(The lattice version of this for staggered fermions is $\langle \bar{\zeta}\zeta(m_\zeta) \rangle = m \sum_t C_\pi(t)$ where $C_\pi(t)$ is the staggered fermion pseudo-Goldstone pion correlator [6].)

Table 2: Fit parameters for fits to the form given in equation (4).

	a_0	a_{-1}	a_1	χ^2
0f	0.00917(23)	$-2.38(53) \times 10^{-6}$	1.669(10)	1.0(17)
2f	0.00765(29)	$-2.61(17) \times 10^{-6}$	1.973(7)	7.6(52)
4f	0.00488(41)	$-3.77(19) \times 10^{-6}$	2.245(15)	15(13)

As shown in [5], the assumption that $\bar{\rho}(\lambda, \beta, m_{\text{dyn}})$ drops dramatically below some λ_{min} and is constant for $\lambda_{\text{min}} < \lambda < \lambda_0$ leads to the result that

$$\langle \bar{\zeta} \zeta(m_\zeta) \rangle = a_0 + a_1 m_\zeta + a_{-1}/m_\zeta + O(m_\zeta^2) + O(m_\zeta^{-2}), \quad (4)$$

for $\lambda_{\text{min}} < m_\zeta < \lambda_0$. Figure 6 shows plots of $\langle \bar{\zeta} \zeta(m_\zeta) \rangle$ for our simulations. The curvature at $m_\zeta \sim 10^{-4}$ is the onset of finite volume effects.

Now, assuming $C(m_\zeta)$ is a smooth function of m_ζ in the range $\lambda_{\text{min}} < m_\zeta < \lambda_0$, we have

$$m_\pi^2 = -\frac{C(0)a_{-1}}{a_0^2} + \left[\frac{C(0)}{a_0} - \frac{C'(0)a_{-1}}{a_0^2} \right] m_\zeta + \dots \quad (5)$$

Thus a non-zero intercept for m_π^2 can be related to the finite volume cutoff in the Dirac eigenvalue spectrum since $a_{-1} \sim -\lambda_{\text{min}}$.

Uncorrelated fits to our measurements of $\langle \bar{\zeta} \zeta \rangle$ are given in Table 2. The error on χ^2 is the jackknifed error on this quantity. For four flavors, we find that a_{-1}/a_0^2 is about 3.6 times as large as the two flavor value, while the ratio of the m_π^2 intercepts is about 5.6. There is clearly some N_f dependence in $C(m_\zeta)$, or higher order terms we have neglected in (5) are important for good quantitative agreement.

This analysis supports the conclusion that we are in a phase with chiral symmetry breaking, although the breaking is small. The small amount of breaking (small a_0) in a finite volume (non-zero a_{-1}) leads to a large intercept for m_π^2 . We are investigating the possible N_f dependence of $C(m_\zeta)$ and are working on a determination of f_π for the four flavor calculation.

5 Conclusions

We have seen that increasing the number of light dynamical quarks to four does alter the valence hadron spectrum at zero temperature. The change in the nucleon to rho mass ratio is about 7% and seems resolved by our statistics. A much larger effect is seen in the amount of chiral symmetry breaking on the lattices. The hadron spectrum exhibits much less chiral symmetry breaking, which is consistent with the suppression of small eigenvalues of the Dirac operator due to the fermionic determinant.

By checking the role of finite volume effects in distorting chiral symmetry breaking, we have argued that our four flavor results are consistent with a chirally asymmetric, confining theory. To gain further evidence for the explanation proposed here, calculations of the explicit eigenvalue density are being done in collaboration with Robert Edwards from SCRI.

Of great interest is whether the effects we have seen for valence calculations done on a dynamical fermion background persist when the dynamical and valence masses are varied together. We are currently undertaking another four flavor calculation at a different dynamical quark mass to gain some insight into this question.

Acknowledgements: We would like to thank Catalin Malareanu for measuring the Wilson lines on our lattices.

References

- [1] D. K. Sinclair, Nucl. Phys. **B** (Proc. Suppl.) **47** (1996) 112; S. Gottlieb, hep-lat/9608107, to appear in the proceedings of Lattice '96.
- [2] D. Chen and R. D. Mawhinney, to appear in the proceedings of Lattice '96, St. Louis, June 1996.
- [3] Dong Chen, Columbia University PhD Thesis, September, 1996.
- [4] F. R. Brown, *et. al.*, Phys. Rev. **D46** (1992) 5655.
- [5] R. D. Mawhinney, Nucl. Phys. **B** (Proc. Suppl.) **47** (1996) 557.
- [6] G. W. Kilcup and S. R. Sharpe, Nucl. Phys. **B283** (1987) 493.

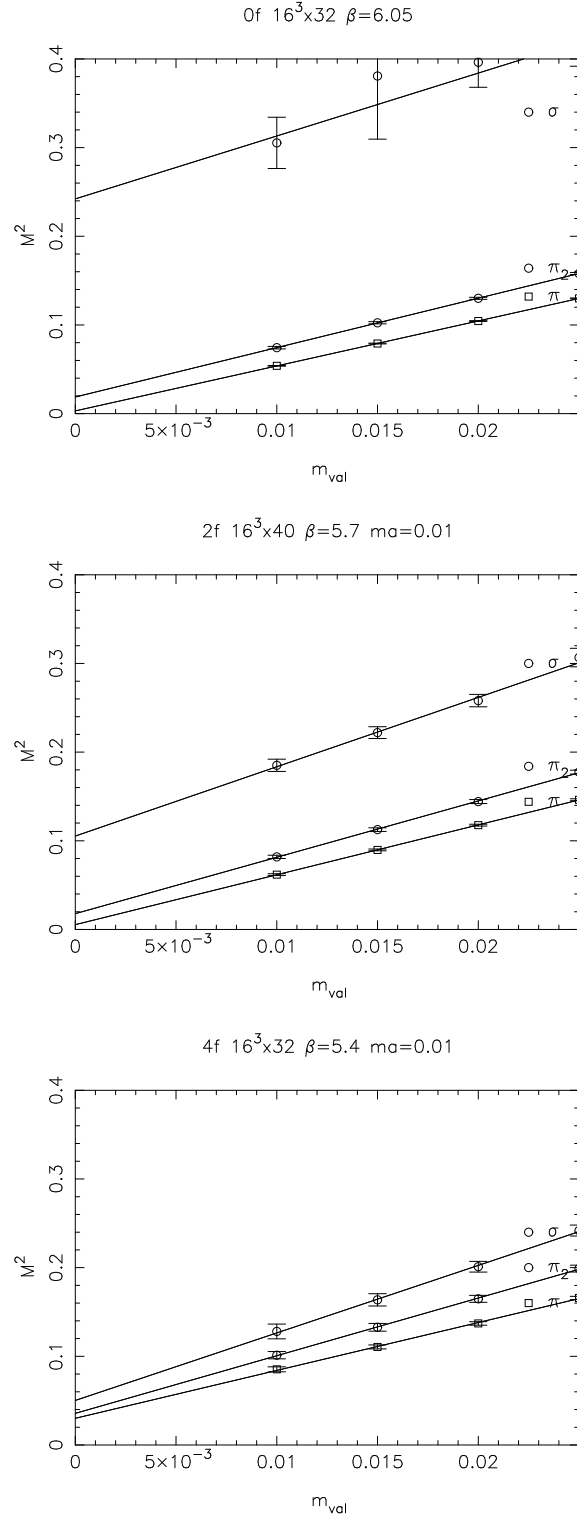


Figure 5: m_π^2 , $m_{\pi_2}^2$ and m_σ^2 vs. m_{val} for the three simulations.

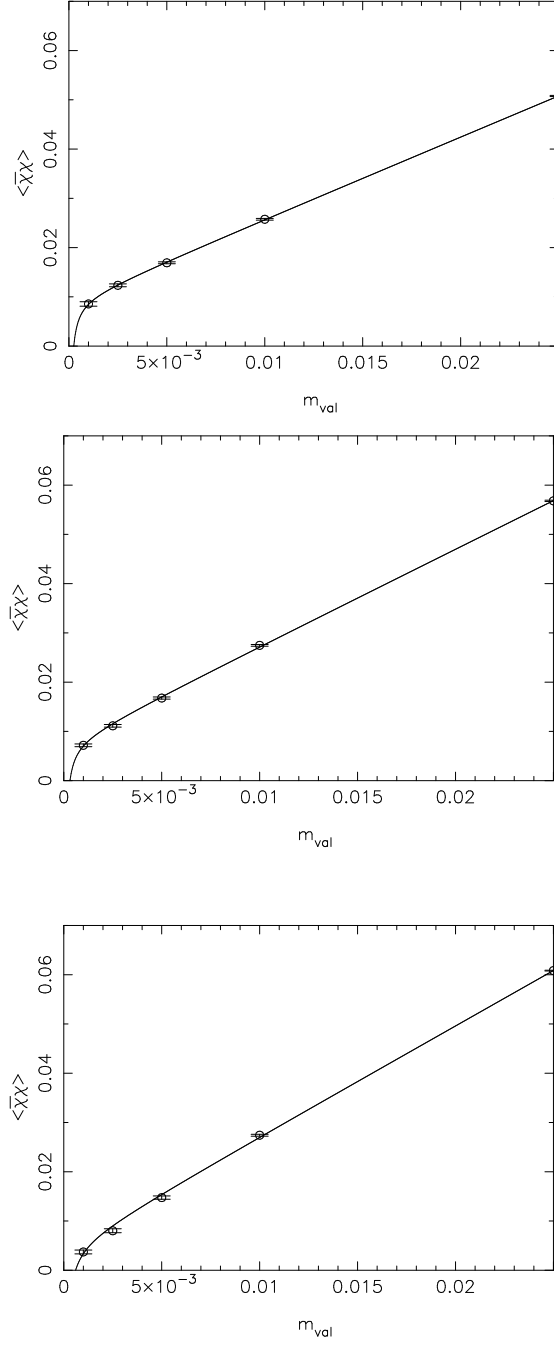


Figure 6: Fits of $\langle \bar{\chi}\chi \rangle$ to the form $a_0 + a_{-1}/m_\chi + a_1 m_\chi$ for five values of m_χ . The top figure is for 0 flavors, the middle for 2 and the bottom for 4.